
Multiple temporal credit assignment rules achieve comparable neural data similarity

Anonymous Author(s)

Affiliation

Address

email

Abstract

1 In the quest to understand how the brain’s learning capabilities stem from its
2 ingredients, developing biologically plausible learning rules presents a promis-
3 ing approach. These rules, often relying on gradient approximations, need to be
4 examined for their effectiveness in areas other than task accuracies. This study
5 assesses whether models trained with biologically plausible learning rules can
6 emulate neural data similarity achieved by models trained with Backpropagation
7 Through Time (BPTT). Employing methods such as Procrustes Analysis, we com-
8 pare well-known neuroscience datasets and discover that models using approximate
9 gradient-based rules show neural data similarities comparable to those trained with
10 BPTT at equal accuracies. Our findings reveal that model architecture and initial
11 conditions have a more pronounced impact on these similarities than the learning
12 rules themselves. Furthermore, our analysis indicates that BPTT-trained models
13 and their biologically plausible counterparts exhibit similar dynamical properties
14 at comparable accuracies. Overall, these results demonstrate the capability of
15 biologically plausible models to not only approximate gradient descent learning
16 in terms of task performance but also emulate its ability to capture neural activity
17 patterns.

18 1 Introduction

19 Understanding how animals learn complex behaviors that span multiple temporal scales is a fun-
20 damental question in neuroscience. Effectively updating synaptic weights to achieve such learning
21 requires solving the temporal credit assignment problem: determining how to assign the contribution
22 of past neural states to future outcomes. In pursuit of answers, neuroscientists have increasingly
23 adopted the mathematical framework of training recurrent neural networks (RNNs) as a model
24 for brain learning mechanisms, inspired by seminal works that have laid the foundation for this
25 approach [1–4]. This pivot has ushered in a variety of biologically plausible (or bio-plausible for
26 short) learning rules, proposing mechanisms by which learning can be achieved using only known
27 biological processes [5, 6]. However, there has been little work on how these proposals connect to
28 neural data, especially in light of the recent growing availability of neural data [7].

29 Navigating the vast space of computational models — which vary not only in learning rules but also in
30 architecture and tasks [6, 8, 9] — necessitates a systematic comparison of model representations with
31 empirical brain data. To address this challenge, a variety of methods have been developed, aiming
32 to quantify the similarity between computational models and neural data. Among these, popular
33 methodologies include linear regression [10], Representational Similarity Analysis (RSA) [11],
34 Centered Kernel Alignment (CKA) [12], Singular Vector Canonical Correlation Analysis [13],
35 Procrustes distance [14–16], and Dynamical Similarity Analysis (DSA) [17]. By comparing the

36 geometry of state representations or the dynamics of neural activity, these methods provide a critical
37 framework for evaluating the extent to which models approximate neural systems.

38 Leveraging existing comparison methodologies, we compute the similarity scores of RNN models
39 trained with bio-plausible learning rules to experimental data. Specifically, we evaluate those
40 similarity scores by comparing them against those achieved by Backpropagation Through Time
41 (BPTT)-trained models. This comparison enables us to assess the efficacy of bio-plausible learning
42 rules as approximations of gradient-descent learning in terms of data similarity. Importantly, the
43 widespread use of task-trained RNNs for modeling brain functions predominantly relies on BPTT [18],
44 despite its bio-plausibility being under scrutiny. It remains an open question whether bio-plausible
45 learning algorithms yield networks with neural similarity comparable to those of BPTT trained
46 networks. Has the pursuit of more biologically plausible learning rules gained biological plausibility
47 at the level of synaptic implementation and parameter updates, but lost biological realism at the level
48 of neural activity?

49 **Main contributions:** Our findings reveal that the distance between data and models trained with
50 truncation-based bio-plausible learning rules is comparable to the distance achieved by models
51 trained using Backpropagation Through Time (BPTT). We specifically focus on learning rules that
52 approximate the gradient by truncating bio-improbable terms, as these truncation-based bio-plausible
53 rules have demonstrated efficacy and versatility in learning non-trivial tasks [19, 20]. Other training
54 strategies for RNNs either face bio-plausibility issues, or have limited success and flexibility on
55 non-trivial tasks (see Related Works in Appendix A). Specifically, our contributions include:

- 56 • First, we benchmark well-known neuroscience datasets (Mante 2013 [4] and Sussillo
57 2015 [21]) using state-of-the-art similarity methods (particularly Procrustes distance) to
58 demonstrate that at equal accuracies, RNNs trained with truncation-based bio-plausible
59 rules achieve a level of similarity to data that is comparable to those trained with their deep
60 learning counterpart, BPTT (Figure 1 and Appendix Figure 7).
- 61 • Second, we further highlight the indistinguishability of different learning rules by demon-
62 strating that the impact of architectural and initial condition variations — particularly initial
63 weight settings — can surpass the differences in Procrustes distances observed across the
64 learning rules (Figure 2).
- 65 • To explain the comparable similarities, we investigate the commonalities between BPTT and
66 its bio-plausible counterparts. Specifically, we demonstrate that BPTT exhibits increased
67 similarity to bio-plausible models at a lower learning rate, as illustrated in Figure 3. Further-
68 more, we analyze their resemblance in terms of the post-training weight eigenspectrum and
69 dynamical properties (explored via DSA) in Appendix Figure 8.

70 2 Results

71 In our study, we analyze the similarity between task-trained RNN models and two neural datasets:
72 Sussillo *et al.*[21] and Mante *et al.*[4]. An overview of our methodology is provided in Figure 1A,
73 with detailed information about our RNN model setup, similarity measure, and datasets in Appendix B.
74 We examine the similarity of RNN models, across different learning rules, to neural data, leveraging
75 Procrustes analysis. Figure 1B shows that multiple learning rules, specifically BPTT and its truncation-
76 based biologically plausible alternative (e-prop), achieve similar Procrustes distances from neural data
77 across two distinct tasks: Sussillo 2015 [21] and Mante 2013 [4]. Although the error bars for BPTT
78 and e-prop do not appear to overlap near perfect accuracy in the Sussillo 2015 task, we demonstrate
79 that such differences are minimal compared to other potential confounding factors in the brain, as
80 shown in Appendix Figure 7.

81 Also, as a sanity check, we verified whether the observed similarity in data proximity is confined
82 to specific learning rules, we also evaluated older learning methods such as node perturbation and
83 evolutionary strategies. Results show that these methods resulted in greater Procrustes distances
84 compared to the aforementioned rules at equivalent accuracy levels, checking that not all learning
85 rules are equally effective. This also indicate the effectiveness of newer bio-plausible gradient-
86 approximating learning rules over some of the older methods (Appendix Figure 9).

87 Additionally, Figure 2 delves into the impact of initial weight settings on model-data distances,
88 revealing that such initial condition nuances exert a more pronounced influence than the choice of

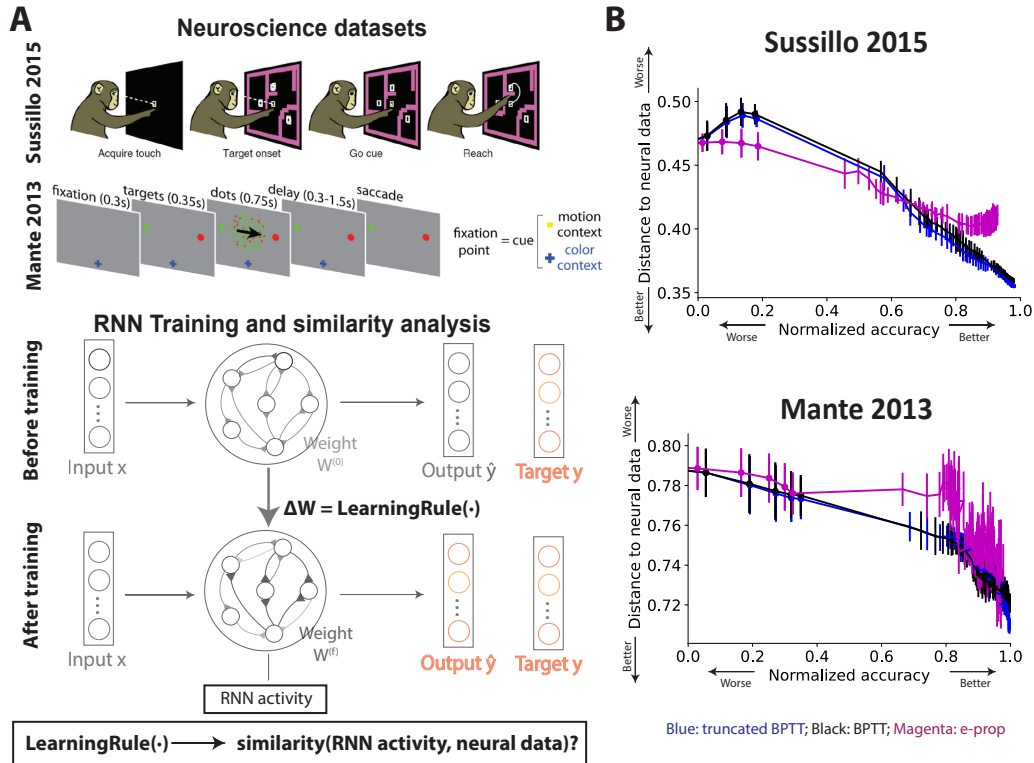


Figure 1: (A) Setup overview: analysis of two neural datasets. We computed similarity scores between RNN activity and electrode recordings from (1) Mante *et al.* (2013) [4] and (2) Sussillo *et al.* (2015) [21]. Schematics have been modified from those in the original papers. RNNs are trained on these respective tasks using various learning rules, including BPTT and bio-plausible alternatives. Subsequently, we evaluate the similarity between RNN activity post-training and the neural recordings to compare model-data similarity across different learning rules. (B) The Procrustes distance vs. accuracy plots for the Sussillo 2015 (top) and Mante 2013 (bottom) tasks illustrate multiple learning rules achieve comparable data similarity. Here, magenta is for e-prop, blue is for truncated BPTT, and black is for BPTT. The mean is plotted with error bars denoting the standard deviations across four different seeds. The x-axis, normalized accuracy, is defined in Appendix B.5. Although there is a slight difference in the distances between e-prop and BPTT at higher accuracies for Sussillo 2015, we demonstrate that such differences are minimal compared to other potential confounding factors in the brain (Figure 2 and Appendix Figure 7).

89 learning rule itself. Initial weight gain is a crucial attribute, as it significantly affects the dynamical
 90 properties of RNNs, particularly the Lyapunov exponents that govern the rates of expansion and
 91 contraction. It can also interpolate between rich and lazy learning regimes, imparting distinct inductive
 92 biases [23–30]. This finding further underscores the significant role of model initialization in shaping
 93 learning outcomes, with particular initial conditions facilitating a closer approximation to neural data
 94 than others.

95 Figure 3 explores the impact of learning rates on model-data distances across learning rules. In
 96 Figure 3A, Procrustes distances remain consistent across learning rates for BPTT. Given that e-prop
 97 can be decomposed into a lower learning rate BPTT and an approximation error [22], which is
 98 further illustrated here by the similarity between a lower learning rate BPTT and e-prop (Figure 3B),
 99 this shared component of a lower learning rate BPTT could partly explain their similar distances.
 100 Additionally, post-training weight eigenspectrums and distances, analyzed via Dynamical Similarity
 101 Analysis (DSA), further reinforce the similarity between BPTT and e-prop (Appendix Figure 8). This
 102 similarity is further explored in Appendix Figure 5, where top demixed principle components show
 103 a qualitative match between the neural data and the models. We also display the similarity among

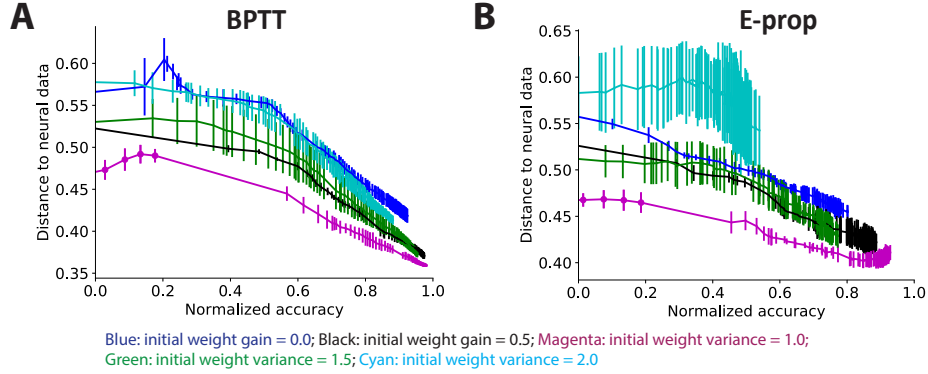


Figure 2: **Impact of Initial Weight Magnitude on Model-Data Distances Exceeds Variation from Learning Rules.** Model-data distances versus normalized accuracy for various initial gain values (depicted by different colors) for (A) BPTT and (B) e-prop. Initial weight gain refers to the multiplier applied to the default initializations for recurrent and readout weights. The results shown are for the Sussillo 2015 task, with similar trends observed for the Mante 2013 task. The mean is plotted with error bars representing the standard deviation.

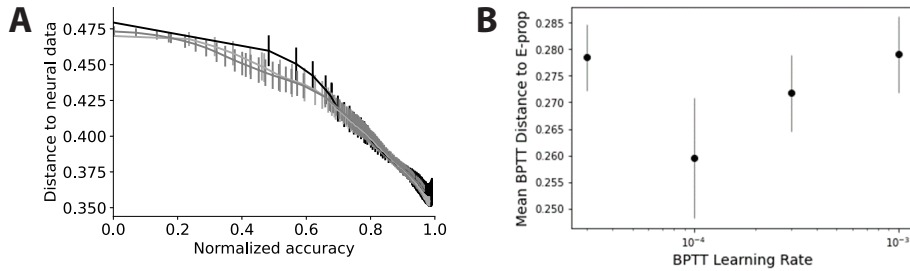


Figure 3: (A) Procrustes distances remain consistent across various learning rates when employing the same rule (BPTT). Different color shades represent different learning rates: $1e-3$, $3e-4$, $1e-4$, and $3e-5$. These rates result in nearly indistinguishable Procrustes distances. The analysis in this figure is done using the Sussillo 2015 task. (B) E-prop — has been viewed as BPTT with a reduced learning rate plus some degree of gradient approximation error [22] — aligns more closely with BPTT at a lower learning rate ($1e-4$) compared to the default setting ($1e-3$). Here, the mean distance from BPTT to e-prop is plotted, with error bars denoting the standard deviation.

104 models in terms of their pairwise distances and their embeddings across different sampled training
 105 snapshots in Appendix Figure 6.

106 It is noteworthy that if all models were equally far from the data, it might also suggest random
 107 noise. However, that is not the case, as our models are significantly closer to the neural data after
 108 training (Figure 4). Additionally, what does it mean for a model to be close to the data? To interpret
 109 model-data closeness, we need a baseline based on data-to-data similarity, which reflects how close
 110 the models are to the data relative to other data points (subsamples within the dataset). Due to limited
 111 subjects, we generated this baseline by splitting the data by neurons, though this may create an
 112 overly stringent baseline due to potential neuron dependence (details in Appendix B.5). For the
 113 Hatsopoulos2007 dataset [31], the final trained models match the neural data as closely as other
 114 neurons (Figure 4). For the Sussillo2015 dataset, trained models approach the noise floor compared
 115 to untrained models; the remaining differences from the baseline offer insights for improving learning
 116 algorithms and architectures in future work.

117 3 Discussion

118 To decipher how the brain’s intricate learning capabilities emerge from its biological processes,
 119 various biologically plausible learning rules have been proposed [6, 5], leaving their connection to

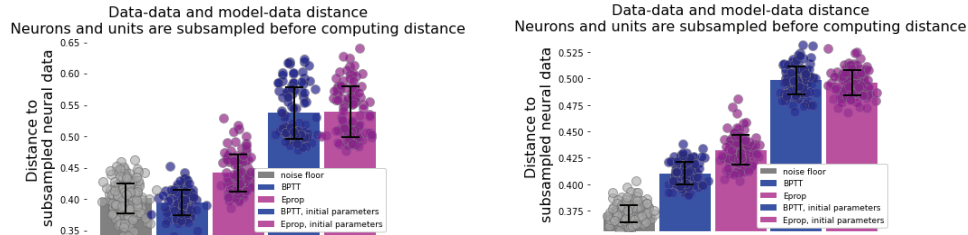


Figure 4: Data-to-data distance (noise floor) vs model-to-model distance (BPTT and e-prop before and after training). Left: Hatsopolous 2007; right: Sussillo 2015. The data-splitting procedure for obtaining the baseline (i.e. noise floor) is detailed in Appendix B.5. We note that these distances are computed with fewer neurons (about half) and units than the previous plots, so the exact distance values here may differ.

120 neural activity as an open question. This study investigates RNN models trained with approximate
 121 gradient-based biologically plausible learning rules, comparing their neural data similarity to models
 122 trained using the standard BPTT algorithm. Grounded in state-of-the-art comparison methods like
 123 Procrustes Analysis, our analysis reveals that at equal accuracies, RNNs employing truncation-based
 124 bio-plausible learning rules exhibit levels of similarity to empirical neural data strikingly comparable
 125 to those achieved by BPTT-trained models (Figures 1 and 2). Further probing into this similarity,
 126 we find that BPTT shows an increased resemblance to bio-plausible models at lower learning rates
 127 (Figure 3), with further examination of their congruence in post-training weight eigenspectrum and
 128 dynamical properties through Dynamical Similarity Analysis (DSA) (Appendix Figure 8). Moreover,
 129 our research reveals that architectural nuances and initial condition variations can significantly
 130 influence model-data similarity, overshadowing the impact of the learning rule choice itself (Figures 2
 131 and 7). Such insights affirm the efficacy of bio-plausible learning rules and encourage a reevaluation
 132 of the factors most critical for aligning model activity with real neural systems.

133 Extending our approach to encompass a broader spectrum of learning rules, architectures, datasets,
 134 and comparison methods is a crucial direction for future research. A comprehensive evaluation
 135 across these dimensions exceeds the scope of a single paper, especially in a rapidly evolving research
 136 landscape. Our study demonstrates the existence of scenarios where biologically plausible rules and
 137 their deep learning counterparts achieve comparable data similarities. Furthermore, our pipeline is
 138 flexible, allowing for expansion across these various facets in future investigations. On the learning
 139 rule front, we primarily examined rules involving gradient truncations, chosen for their biological
 140 plausibility, proven efficacy in task learning, and versatility in settings that eschew the equilibrium
 141 assumption [32, 33], as detailed in the Related Works section in Appendix A. These rules have been
 142 the subject of several recent studies within the computational neuroscience community [34, 22].
 143 Additionally, our analysis is predicated on the concept of learning through synaptic credit assignment,
 144 yet other approaches — e.g. in-context learning [35] if it can be implemented biologically — warrant
 145 future examination. In addition to learning rules, other model attributes — particularly architecture
 146 and initialization, as illustrated in Figure 2 — are crucial areas for future research. Although our
 147 results demonstrate comparable similarities at equal accuracies, this does not imply that e-prop is
 148 indistinguishable from BPTT. In fact, e-prop accuracies falls short on some of the more challenging
 149 tasks [36]. Future experimental neuroscience research could focus on obtaining data from these
 150 challenging tasks where e-prop training fails to perform well and conduct further comparisons using
 151 these tasks. Furthermore, we chose to focus on Procrustes distance for its ability to provide a proper
 152 metric for comparing the geometry of state representations, and its stringency in only allowing for
 153 rotations and a global stretching to align neural trajectories. We were also motivated to emphasize
 154 Procrustes distance because several weaknesses have been identified in other similarity measures that
 155 are, for example, biased due to high dimensionality, or may rely on low variance noise components
 156 of the data [12, 37–39]. That said, like all scalar measures, it focuses on specific structures, and it
 157 remains uncertain whether these structures accurately capture the computational properties of interest.
 158 Therefore, developing new measures remains a crucial and intriguing endeavor [40–45]. Altogether,
 159 this vibrant area — which focuses on comparing neurally plausible learning rules with neural data —
 160 is ripe for exploration across various knobs including learning rules, architecture, tasks/datasets, and
 161 comparison methodologies.

References

- 162
- 163 [1] David Zipser. Recurrent network model of the neural mechanism of short-term active memory.
164 *Neural Computation*, 3(2):179–193, 1991.
- 165 [2] Eberhard Fetz. Are movement parameters recognizably coded in the activity of single neurons?,
166 1992.
- 167 [3] Sohie Lee Moody, Steven P. Wise, Giuseppe di Pellegrino, and David Zipser. A model that
168 accounts for activity in primate frontal cortex during a delayed matching-to-sample task. *Journal*
169 *of Neuroscience*, 18(1):399–410, 1998.
- 170 [4] Valerio Mante, David Sussillo, Krishna V Shenoy, and William T Newsome. Context-dependent
171 computation by recurrent dynamics in prefrontal cortex. *nature*, 503(7474):78–84, 2013.
- 172 [5] Timothy P Lillicrap, Adam Santoro, Luke Marris, Colin J Akerman, and Geoffrey Hinton.
173 Backpropagation and the brain. *Nature Reviews Neuroscience*, 21(6):335–346, 2020.
- 174 [6] Blake A Richards, Timothy P Lillicrap, Philippe Beaudoin, Yoshua Bengio, Rafal Bogacz,
175 Amelia Christensen, Claudia Clopath, Rui Ponte Costa, Archy de Berker, Surya Ganguli, et al.
176 A deep learning framework for neuroscience. *Nature neuroscience*, 22(11):1761–1770, 2019.
- 177 [7] Christof Koch, Karel Svoboda, Amy Bernard, Michele A Basso, Anne K Churchland, Adri-
178 enne L Fairhall, Peter A Groblewski, Jérôme A Lecoq, Zachary F Mainen, Mackenzie W Mathis,
179 et al. Next-generation brain observatories. *Neuron*, 110(22):3661–3666, 2022.
- 180 [8] Anthony M Zador. A critique of pure learning and what artificial neural networks can learn
181 from animal brains. *Nature communications*, 10(1):1–7, 2019.
- 182 [9] Guangyu Robert Yang and Manuel Molano Mazon. Next-generation of recurrent neural network
183 models for cognition. 2021.
- 184 [10] Daniel LK Yamins, Ha Hong, Charles F Cadieu, Ethan A Solomon, Darren Seibert, and James J
185 DiCarlo. Performance-optimized hierarchical models predict neural responses in higher visual
186 cortex. *Proceedings of the national academy of sciences*, 111(23):8619–8624, 2014.
- 187 [11] Nikolaus Kriegeskorte, Marieke Mur, and Peter A Bandettini. Representational similarity
188 analysis-connecting the branches of systems neuroscience. *Frontiers in systems neuroscience*,
189 2:249, 2008.
- 190 [12] Simon Kornblith, Mohammad Norouzi, Honglak Lee, and Geoffrey Hinton. Similarity of neural
191 network representations revisited. In *International conference on machine learning*, pages
192 3519–3529. PMLR, 2019.
- 193 [13] Maithra Raghu, Justin Gilmer, Jason Yosinski, and Jascha Sohl-Dickstein. Svcca: Singular
194 vector canonical correlation analysis for deep learning dynamics and interpretability. *Advances*
195 *in neural information processing systems*, 30, 2017.
- 196 [14] Alex H Williams, Erin Kunz, Simon Kornblith, and Scott Linderman. Generalized shape metrics
197 on neural representations. *Advances in Neural Information Processing Systems*, 34:4738–4750,
198 2021.
- 199 [15] Frances Ding, Jean-Stanislas Denain, and Jacob Steinhardt. Grounding representation similarity
200 through statistical testing. *Advances in Neural Information Processing Systems*, 34:1556–1568,
201 2021.
- 202 [16] Lyndon R Duong, Jingyang Zhou, Josue Nassar, Jules Berman, Jeroen Olieslagers, and Alex H
203 Williams. Representational dissimilarity metric spaces for stochastic neural networks. *arXiv*
204 *preprint arXiv:2211.11665*, 2022.
- 205 [17] Mitchell Ostrow, Adam Eisen, Leo Kozachkov, and Ila Fiete. Beyond geometry: Comparing
206 the temporal structure of computation in neural circuits with dynamical similarity analysis.
207 *Advances in Neural Information Processing Systems*, 36, 2024.

- 208 [18] Guangyu Robert Yang and Xiao-Jing Wang. Artificial neural networks for neuroscientists: a
209 primer. *Neuron*, 107(6):1048–1070, 2020.
- 210 [19] Guillaume Bellec, Franz Scherr, Anand Subramoney, Elias Hajek, Darjan Salaj, Robert Leg-
211 enstein, and Wolfgang Maass. A solution to the learning dilemma for recurrent networks of
212 spiking neurons. *Nature communications*, 11(1):3625, 2020.
- 213 [20] Roy Henha Eyono, Ellen Boven, Arna Ghosh, Joseph Pemberton, Franz Scherr, Claudia Clopath,
214 Rui Ponte Costa, Wolfgang Maass, Blake A Richards, Cristina Savin, et al. Current state and
215 future directions for learning in biological recurrent neural networks: A perspective piece.
216 *Neurons, Behavior, Data analysis, and Theory*, 1, 2022.
- 217 [21] David Sussillo, Mark M Churchland, Matthew T Kaufman, and Krishna V Shenoy. A neural net-
218 work that finds a naturalistic solution for the production of muscle activity. *Nature neuroscience*,
219 18(7):1025–1033, 2015.
- 220 [22] Yuhan Helena Liu, Arna Ghosh, Blake A Richards, Eric Shea-Brown, and Guillaume Lajoie.
221 Beyond accuracy: generalization properties of bio-plausible temporal credit assignment rules.
222 *arXiv preprint arXiv:2206.00823*, 2022.
- 223 [23] Lukas Braun, Clémentine Dominé, James Fitzgerald, and Andrew Saxe. Exact learning dynam-
224 ics of deep linear networks with prior knowledge. *Advances in Neural Information Processing*
225 *Systems*, 35:6615–6629, 2022.
- 226 [24] Timo Flesch, Andrew Saxe, and Christopher Summerfield. Continual task learning in natural
227 and artificial agents. *Trends in Neurosciences*, 46(3):199–210, 2023.
- 228 [25] Lenaic Chizat, Edouard Oyallon, and Francis Bach. On lazy training in differentiable program-
229 ming. *Advances in Neural Information Processing Systems*, 32, 2019.
- 230 [26] Blake Woodworth, Suriya Gunasekar, Jason D Lee, Edward Moroshko, Pedro Savarese, Itay
231 Golan, Daniel Soudry, and Nathan Srebro. Kernel and rich regimes in overparametrized models.
232 In *Conference on Learning Theory*, pages 3635–3673. PMLR, 2020.
- 233 [27] Friedrich Schuessler, Francesca Mastrogiuseppe, Srdjan Ostojic, and Omri Barak. Aligned and
234 oblique dynamics in recurrent neural networks. *arXiv preprint arXiv:2307.07654*, 2023.
- 235 [28] Blake Bordelon and Cengiz Pehlevan. The influence of learning rule on representation dynamics
236 in wide neural networks. *arXiv preprint arXiv:2210.02157*, 2022.
- 237 [29] Yuhan Helena Liu, Aristide Baratin, Jonathan Cornford, Stefan Mihalas, Eric Shea-Brown, and
238 Guillaume Lajoie. How connectivity structure shapes rich and lazy learning in neural circuits.
239 *arXiv preprint arXiv:2310.08513*, 2023.
- 240 [30] Jonas Paccolat, Leonardo Petrini, Mario Geiger, Kevin Tyloo, and Matthieu Wyart. Geometric
241 compression of invariant manifolds in neural networks. *Journal of Statistical Mechanics: Theory*
242 *and Experiment*, 2021(4):044001, 2021.
- 243 [31] Nicholas G Hatsopoulos, Qingqing Xu, and Yali Amit. Encoding of movement fragments in the
244 motor cortex. *Journal of Neuroscience*, 27(19):5105–5114, 2007.
- 245 [32] Benjamin Scellier and Yoshua Bengio. Equilibrium propagation: Bridging the gap between
246 energy-based models and backpropagation. *Frontiers in computational neuroscience*, 11:24,
247 2017.
- 248 [33] Alexander Meulemans, Nicolas Zucchet, Seijin Kobayashi, Johannes Von Oswald, and João
249 Sacramento. The least-control principle for local learning at equilibrium. *Advances in Neural*
250 *Information Processing Systems*, 35:33603–33617, 2022.
- 251 [34] Jacob Portes, Christian Schmid, and James M Murray. Distinguishing learning rules with brain
252 machine interfaces. *Advances in neural information processing systems*, 35:25937–25950,
253 2022.

- 254 [35] Johannes Von Oswald, Eyvind Niklasson, Ettore Randazzo, João Sacramento, Alexander
255 Mordvintsev, Andrey Zhmoginov, and Max Vladymyrov. Transformers learn in-context by
256 gradient descent. In *International Conference on Machine Learning*, pages 35151–35174.
257 PMLR, 2023.
- 258 [36] Yuhan Helena Liu, Stephen Smith, Stefan Mihalas, Eric Shea-Brown, and Uygar Sümbül. Cell-
259 type-specific neuromodulation guides synaptic credit assignment in a spiking neural network.
260 *Proceedings of the National Academy of Sciences*, 118(51):e2111821118, 2021.
- 261 [37] MohammadReza Davari, Stefan Horoi, Amine Natik, Guillaume Lajoie, Guy Wolf, and Eugene
262 Belilovsky. Reliability of cka as a similarity measure in deep learning, 2022.
- 263 [38] Marin Dujmović, Jeffrey S Bowers, Federico Adolphi, and Gaurav Malhotra. Obstacles to
264 inferring mechanistic similarity using representational similarity analysis. *bioRxiv*, 2023.
- 265 [39] Eric Elmoznino and Michael F. Bonner. High-performing neural network models of visual
266 cortex benefit from high latent dimensionality. *PLOS Computational Biology*, 20(1):1–23, 01
267 2024.
- 268 [40] Nicholas J. Sexton and Bradley C. Love. Reassessing hierarchical correspondences between
269 brain and deep networks through direct interface. *Science Advances*, 8(28):eabm2219, 2022.
- 270 [41] Iliia Sucholutsky, Lukas Muttenthaler, Adrian Weller, Andi Peng, Andreea Bobu, Been Kim,
271 Bradley C Love, Erin Grant, Jascha Achterberg, Joshua B Tenenbaum, et al. Getting aligned on
272 representational alignment. *arXiv preprint arXiv:2310.13018*, 2023.
- 273 [42] Baihan Lin and Nikolaus Kriegeskorte. The topology and geometry of neural representations,
274 2023.
- 275 [43] Max Klabunde, Tobias Schumacher, Markus Strohmaier, and Florian Lemmerich. Similarity of
276 neural network models: A survey of functional and representational measures, 2023.
- 277 [44] Jeffrey S. Bowers, Gaurav Malhotra, Marin Dujmović, Milton Llera Montero, Christian
278 Tsvetkov, Valerio Biscione, Guillermo Puebla, Federico Adolphi, John E. Hummel, Rachel F.
279 Heaton, and et al. Deep problems with neural network models of human vision. *Behavioral and*
280 *Brain Sciences*, 46:e385, 2023.
- 281 [45] Andrew Kyle Lampinen, Stephanie C. Y. Chan, and Katherine Hermann. Learned feature
282 representations are biased by complexity, learning order, position, and more, 2024.
- 283 [46] Geoffrey Hinton. The forward-forward algorithm: Some preliminary investigations. *arXiv*
284 *preprint arXiv:2212.13345*, 2022.
- 285 [47] Axel Laborieux and Friedemann Zenke. Holomorphic equilibrium propagation computes exact
286 gradients through finite size oscillations. *arXiv preprint arXiv:2209.00530*, 2022.
- 287 [48] Will Greedy, Heng Wei Zhu, Joseph Pemberton, Jack Mellor, and Rui Ponte Costa. Single-phase
288 deep learning in cortico-cortical networks. *Advances in Neural Information Processing Systems*,
289 35:24213–24225, 2022.
- 290 [49] João Sacramento, Rui Ponte Costa, Yoshua Bengio, and Walter Senn. Dendritic cortical
291 microcircuits approximate the backpropagation algorithm. *arXiv preprint arXiv:1810.11393*,
292 2018.
- 293 [50] Alexandre Payeur, Jordan Guerguiev, Friedemann Zenke, Blake A Richards, and Richard Naud.
294 Burst-dependent synaptic plasticity can coordinate learning in hierarchical circuits. *Nature*
295 *neuroscience*, pages 1–10, 2021.
- 296 [51] Pieter R Roelfsema and Anthony Holtmaat. Control of synaptic plasticity in deep cortical
297 networks. *Nature Reviews Neuroscience*, 19(3):166–180, 2018.
- 298 [52] Johnatan Aljadeff, James D’amour, Rachel E Field, Robert C Froemke, and Claudia Clopath.
299 Cortical credit assignment by hebbian, neuromodulatory and inhibitory plasticity. *arXiv preprint*
300 *arXiv:1911.00307*, 2019.

- 301 [53] James M Murray. Local online learning in recurrent networks with random feedback. *Elife*,
302 8:e43299, 2019.
- 303 [54] Yuhan Helena Liu, Stephen Smith, Stefan Mihalas, Eric Shea-Brown, and Uygur Sümbül.
304 Biologically-plausible backpropagation through arbitrary timespans via local neuromodulators.
305 *arXiv preprint arXiv:2206.01338*, 2022.
- 306 [55] Owen Marschall, Kyunghyun Cho, and Cristina Savin. A unified framework of online learning
307 algorithms for training recurrent neural networks. *The Journal of Machine Learning Research*,
308 21(1):5320–5353, 2020.
- 309 [56] Arna Ghosh, Yuhan Helena Liu, Guillaume Lajoie, Konrad Kording, and Blake Aaron Richards.
310 How gradient estimator variance and bias impact learning in neural networks. In *The Eleventh*
311 *International Conference on Learning Representations*, 2023.
- 312 [57] Basile Confavreux, Poornima Ramesh, Pedro J Goncalves, Jakob H Macke, and Tim Vogels.
313 Meta-learning families of plasticity rules in recurrent spiking networks using simulation-based
314 inference. *Advances in Neural Information Processing Systems*, 36, 2024.
- 315 [58] Aran Nayebi, Sanjana Srivastava, Surya Ganguli, and Daniel L Yamins. Identifying learning
316 rules from neural network observables. *Advances in Neural Information Processing Systems*,
317 33:2639–2650, 2020.
- 318 [59] Zoe Ashwood, Nicholas A Roy, Ji Hyun Bak, and Jonathan W Pillow. Inferring learning
319 rules from animal decision-making. *Advances in Neural Information Processing Systems*,
320 33:3442–3453, 2020.
- 321 [60] Sukbin Lim, Jillian L McKee, Luke Woloszyn, Yali Amit, David J Freedman, David L Sheinberg,
322 and Nicolas Brunel. Inferring learning rules from distributions of firing rates in cortical neurons.
323 *Nature neuroscience*, 18(12):1804–1810, 2015.
- 324 [61] Daniel R Kepple, Rainer Engelken, and Kanaka Rajan. Curriculum learning as a tool to uncover
325 learning principles in the brain. In *International Conference on Learning Representations*, 2021.
- 326 [62] Saurabh Vyas, Matthew D Golub, David Sussillo, and Krishna V Shenoy. Computation through
327 neural population dynamics. *Annual Review of Neuroscience*, 43:249–275, 2020.
- 328 [63] Matthew G Perich, Charlotte Arlt, Sofia Soares, Megan E Young, Clayton P Mosher, Juri Minxha,
329 Eugene Carter, Ueli Rutishauser, Peter H Rudebeck, Christopher D Harvey, et al. Inferring
330 brain-wide interactions using data-constrained recurrent neural network models. *bioRxiv*, pages
331 2020–12, 2021.
- 332 [64] Friedrich Schuessler, Francesca Mastrogiuseppe, Alexis Dubreuil, Srdjan Ostojic, and Omri
333 Barak. The interplay between randomness and structure during learning in rnns. *Advances in*
334 *neural information processing systems*, 33:13352–13362, 2020.
- 335 [65] Guangyu Robert Yang, Madhura R Joglekar, H Francis Song, William T Newsome, and Xiao-
336 Jing Wang. Task representations in neural networks trained to perform many cognitive tasks.
337 *Nature neuroscience*, 22(2):297–306, 2019.
- 338 [66] Elia Turner, Kabir V Dabholkar, and Omri Barak. Charting and navigating the space of
339 solutions for recurrent neural networks. *Advances in Neural Information Processing Systems*,
340 34:25320–25333, 2021.
- 341 [67] Adrian Valente, Srdjan Ostojic, and Jonathan Pillow. Probing the relationship between
342 linear dynamical systems and low-rank recurrent neural network models. *arXiv preprint*
343 *arXiv:2110.09804*, 2021.
- 344 [68] Christopher Langdon and Tatiana A Engel. Latent circuit inference from heterogeneous neural
345 responses during cognitive tasks. *bioRxiv*, 2022.
- 346 [69] Omri Barak. Recurrent neural networks as versatile tools of neuroscience research. *Current*
347 *opinion in neurobiology*, 46:1–6, 2017.

- 348 [70] H Francis Song, Guangyu R Yang, and Xiao-Jing Wang. Training excitatory-inhibitory recurrent
349 neural networks for cognitive tasks: a simple and flexible framework. *PLoS computational*
350 *biology*, 12(2):e1004792, 2016.
- 351 [71] Niru Maheswaranathan, Alex Williams, Matthew Golub, Surya Ganguli, and David Sussillo.
352 Universality and individuality in neural dynamics across large populations of recurrent networks.
353 *Advances in neural information processing systems*, 32, 2019.
- 354 [72] Stephen J. Smith, Michael Hawrylycz, Jean Rossier, and Uygur Sümbül. New light on cortical
355 neuropeptides and synaptic network plasticity. *Current Opinion in Neurobiology*, 63:176–188,
356 aug 2020.
- 357 [73] Jacob Menick, Erich Elsen, Utku Evci, Simon Osindero, Karen Simonyan, and Alex Graves. A
358 practical sparse approximation for real time recurrent learning. *arXiv preprint arXiv:2006.07232*,
359 2020.
- 360 [74] David Sussillo and Larry F Abbott. Generating coherent patterns of activity from chaotic neural
361 networks. *Neuron*, 63(4):544–557, 2009.
- 362 [75] Thomas Miconi. Biologically plausible learning in recurrent neural networks reproduces neural
363 dynamics observed during cognitive tasks. *Elife*, 6:e20899, 2017.
- 364 [76] SueYeon Chung and Larry F Abbott. Neural population geometry: An approach for understand-
365 ing biological and artificial neural networks. *Current opinion in neurobiology*, 70:137–144,
366 2021.
- 367 [77] Martin Schrimpf, Jonas Kubilius, Ha Hong, Najib J Majaj, Rishi Rajalingham, Elias B Issa,
368 Kohitij Kar, Pouya Bashivan, Jonathan Prescott-Roy, Franziska Geiger, et al. Brain-score:
369 Which artificial neural network for object recognition is most brain-like? *BioRxiv*, page 407007,
370 2018.
- 371 [78] Rishidev Chaudhuri, Berk Gerçek, Biraj Pandey, Adrien Peyrache, and Ila Fiete. The intrinsic
372 attractor manifold and population dynamics of a canonical cognitive circuit across waking and
373 sleep. *Nature neuroscience*, 22(9):1512–1520, 2019.
- 374 [79] Marino Pagan, Vincent D Tang, Mikio C Aoi, Jonathan W Pillow, Valerio Mante, David
375 Sussillo, and Carlos D Brody. A new theoretical framework jointly explains behavioral and
376 neural variability across subjects performing flexible decision-making. *bioRxiv*, pages 2022–11,
377 2022.
- 378 [80] Alan D Degenhart, William E Bishop, Emily R Oby, Elizabeth C Tyler-Kabara, Steven M Chase,
379 Aaron P Batista, and Byron M Yu. Stabilization of a brain–computer interface via the alignment
380 of low-dimensional spaces of neural activity. *Nature biomedical engineering*, 4(7):672–685,
381 2020.
- 382 [81] Mahdiyar Shahbazi, Ali Shirali, Hamid Aghajan, and Hamed Nili. Using distance on the riemannian
383 manifold to compare representations in brain and in models. *NeuroImage*, 239:118271,
384 2021.
- 385 [82] Meenakshi Khosla and Alex H Williams. Soft matching distance: A metric on neural represen-
386 tations that captures single-neuron tuning. *arXiv preprint arXiv:2311.09466*, 2023.
- 387 [83] Baihan Lin and Nikolaus Kriegeskorte. The topology and geometry of neural representations.
388 *arXiv preprint arXiv:2309.11028*, 2023.
- 389 [84] Dean A Pospisil, Brett W Larsen, Sarah E Harvey, and Alex H Williams. Estimating shape
390 distances on neural representations with limited samples. *arXiv preprint arXiv:2310.05742*,
391 2023.
- 392 [85] Jeffrey C. Magee and Christine Grienberger. Synaptic Plasticity Forms and Functions. *Annual*
393 *Review of Neuroscience*, 43(1):95–117, jul 2020.
- 394 [86] Wulfram Gerstner, Marco Lehmann, Vasiliki Liakoni, Dane Corneil, and Johanni Brea. Eligi-
395 bility Traces and Plasticity on Behavioral Time Scales: Experimental Support of NeoHebbian
396 Three-Factor Learning Rules. *Frontiers in Neural Circuits*, 12:53, jul 2018.

- 397 [87] Sarah E Harvey, Brett W. Larsen, and Alex H Williams. Duality of bures and shape distances
398 with implications for comparing neural representations. In *UniReps: the First Workshop on*
399 *Unifying Representations in Neural Models*, 2023.
- 400 [88] Manuel Molano-Mazon, Joao Barbosa, Jordi Pastor-Ciurana, Marta Fradera, Ru-Yuan Zhang,
401 Jeremy Forest, Jorge del Pozo Lerida, Li Ji-An, Christopher J Cueva, Jaime de la Rocha, et al.
402 Neurogym: An open resource for developing and sharing neuroscience tasks. 2022.
- 403 [89] Justin Werfel, Xiaohui Xie, and H Seung. Learning curves for stochastic gradient descent in
404 linear feedforward networks. *Advances in neural information processing systems*, 16, 2003.
- 405 [90] Timothy P Lillicrap, Daniel Cownden, Douglas B Tweed, and Colin J Akerman. Random synap-
406 tic feedback weights support error backpropagation for deep learning. *Nature communications*,
407 7(1):1–10, 2016.
- 408 [91] Tim Salimans, Jonathan Ho, Xi Chen, Szymon Sidor, and Ilya Sutskever. Evolution strategies
409 as a scalable alternative to reinforcement learning. *arXiv preprint arXiv:1703.03864*, 2017.
- 410 [92] Nathan Cloos, Moufan Li, Guangyu Robert Yang, and Christopher J Cueva. Scaling up the
411 evaluation of recurrent neural network models for cognitive neuroscience. 2022.
- 412 [93] Adam Paszke, Sam Gross, Francisco Massa, Adam Lerer, James Bradbury, Gregory Chanan,
413 Trevor Killeen, Zeming Lin, Natalia Gimelshein, Luca Antiga, et al. Pytorch: An imperative
414 style, high-performance deep learning library. *Advances in neural information processing*
415 *systems*, 32, 2019.
- 416 [94] Brian DePasquale, Christopher J Cueva, Kanaka Rajan, G Sean Escola, and LF Abbott. full-
417 force: A target-based method for training recurrent networks. *PloS one*, 13(2):e0191527,
418 2018.

420 Understanding the mechanisms through which the brain learns, utilizing its myriad elements, remains
421 a perennial quest in neuroscience. Recent years have seen a resurgence of interest in proposing
422 biologically plausible learning rules [5, 32, 46–52, 33, 53, 19, 36, 54–57, 6], suggesting potential
423 neural algorithms that leverage known neural components. Despite these advances, relatively little
424 research has focused on how such proposals might connect back to neural circuits. A prevailing line
425 of work concentrates on inferring learning rules directly from neural data [58–61, 34]. In contrast, our
426 approach evaluates different learning rules based on their post-learning activity similarity to neural
427 data, offering a flexible methodology that prioritizes the outcome of learning without necessitating
428 data from before or during the training process.

429 Our research focuses on learning rules for recurrent neural networks (RNNs), which are extensively
430 used in brain modeling [62–65, 4, 66–71, 9]. This study specifically investigates local learning rules
431 that truncate gradients, as these have shown promising results in task learning and offer versatility
432 across various network architectures. A systematic review [55] recognized random feedback local
433 online (RFLO) as the only fully local (hence bio-plausible) rule. Post-review developments include
434 e-prop, an adaptation of RFLO for non-vanilla (particularly spike-based) RNNs [19], and MDGL [36]
435 with its extension ModProp [54], which further refine the gradient approximation by considering
436 local modulatory signals [72]. These rules are notable for their effectiveness in bio-plausible temporal
437 credit assignment, matching the performance of the more traditional backpropagation through time
438 (BPTT) in many settings [20]. Our study will, therefore, concentrate on these specific learning rules
439 due to their demonstrated efficacy and bio-plausibility. Further details of these rules are explained in
440 Appendix B.4.

441 Alternative training strategies for RNNs exist, but they either face bio-plausibility issues, lack
442 versatility across settings, or struggle to scale to complex tasks. For instance, equilibrium propagation
443 and related rules depend on the equilibrium assumption [32, 33]. Within truncation-based methods,
444 the SnAp- n algorithm introduced in [73] allows customization by selecting the truncation level n .
445 While SnAp-1 aligns closely with e-prop/RFLO, SnAp-2 and higher n require storing a triple tensor,
446 which poses $O(N^3)$ storage demands not yet proven feasible for neural circuits. Therefore, SnAp- n
447 ($n \geq 2$) remains biologically implausible, while SnAp-1 effectively reduces to e-prop/RFLO under
448 certain conditions. Beyond truncation, the KeRNL algorithm approximates long-term dependencies
449 using first-order low-pass filters and updates parameters via node perturbation, yet this also challenges
450 biological plausibility by requiring frequent meta-parameter updates. Other strategies like FORCE
451 learning [74] offer alternatives, but our scope assumes recurrent weight adjustment and the non-
452 reservoir version faces issues with locality. This study focuses on supervised learning, setting aside
453 the broader field of reinforcement learning for future work, thus not covering certain learning rules
454 like the one in [75].

455 Comparing high-dimensional neural responses across different systems and contexts is crucial in
456 neuroscience [76] for assessing model quality, determining invariant neural states, and aligning
457 brain-machine interface recordings, among other tasks [77–80]. Among the myriad of methods
458 developed to quantify representational dissimilarity [10, 77, 11, 13, 81, 14–16, 82–84] — such
459 as linear regression, Canonical Correlation Analysis (CCA), Centered Kernel Alignment (CKA),
460 Representational Similarity Analysis (RSA), shape metrics, and Riemannian distance — we focus
461 on Procrustes distance for its ability to provide a proper metric for comparing the geometry of state
462 representations, and because several weaknesses have been identified in other similarity measures that
463 are, for example, biased due to high dimensionality, or may rely on low variance noise components
464 of the data [12, 37–39]. Additionally, we extend our investigation to include Dynamical Similarity
465 Analysis (DSA [17]) in the Appendix, assessing system dynamics to complement our geometric
466 analyses. Overall, the value of these existing measures stems from their ability to compare complex
467 systems without fully understanding them by capturing key structures. However, this strength also
468 poses a limitation: they focus on specific structures, and it remains uncertain whether these structures
469 accurately capture the computational properties of interest. Therefore, developing new measures
470 remains a crucial and intriguing endeavor [40–45].

471 **B Methods**

472 **B.1 RNN training setup**

473 Our RNN architecture consists of N_{in} input units, N hidden units, and N_{out} readout units. The
 474 update mechanism for the hidden state at time t , $h_t \in \mathbb{R}^N$, follows the equation:

$$h_{t+1} = \beta h_t + (1 - \beta)(W_h f(h_t) + W_x x_t), \quad (1)$$

475 where $\beta = 1 - \frac{dt}{\tau_m} \in \mathbb{R}$ is the leak factor determined by the simulation time step dt and membrane
 476 time constant τ_m ; $f(\cdot) : \mathbb{R}^N \rightarrow \mathbb{R}^N$ represents the *retanh* activation function; $W_h \in \mathbb{R}^{N \times N}$ and
 477 $W_x \in \mathbb{R}^{N \times N_{in}}$ are the recurrent and input weight matrices, respectively; and $x_t \in \mathbb{R}^{N_{in}}$ is the
 478 input at time t . The readout, $\hat{y}_t \in \mathbb{R}^{N_{out}}$, is calculated as a linear combination of the hidden state’s
 479 activation, $f(h_t)$, with the readout weights $w \in \mathbb{R}^{N_{out} \times N}$.

480 To train this RNN for the specific tasks in the datasets, we used synthetic input and target output
 481 detailed in Appendix B.4. Our objective is to minimize the scalar loss $L \in \mathbb{R}$. For loss minimization,
 482 we examine various learning rules, including BPTT (our benchmark) that computes the exact gradient,
 483 $\nabla_W L(W_h) \in \mathbb{R}^{N \times (N_{in} + N + N_{out})}$, as well as bio-plausible learning rules that apply approximate
 484 gradients, $\tilde{\nabla}_W L(W) \in \mathbb{R}^{N \times (N_{in} + N + N_{out})}$:

$$\Delta W = -\eta \nabla_W L(W), \quad (2)$$

485

$$\widehat{\Delta W} = -\eta \tilde{\nabla}_W L(W), \quad (3)$$

486 where $W = [W_h \ W_x \ w^T] \in \mathbb{R}^{N \times (N_{in} + N + N_{out})}$ encompasses all trainable parameters and
 487 $\eta \in \mathbb{R}$ is the learning rate.

488 The learning rules investigated in this study are elaborated upon in Appendix B.4. Our analysis
 489 centers on how training RNNs with different algorithms influences their similarity to neural data.
 490 Predominantly, we concentrate on the truncation-based, bio-plausible rule known as e-prop [19],
 491 which simplifies the gradient by retaining only those terms that align with a three-factor learning
 492 rule. This includes a Hebbian eligibility trace modulated by a top-down instructive factor, potentially
 493 attributable to neuromodulators [85, 86]. It is noteworthy that e-prop is equivalent to the RFLO
 494 learning rule introduced in [53] under most conditions. Additionally, we explore ModProp [54],
 495 which incorporates cell-type-specific local modulatory signals [72] to recover terms omitted by e-prop.
 496 However, due to ModProp’s limitations (it is constrained to settings that adhere to Dale’s law and
 497 employ the *ReLU* activation function), our examination of this rule is restricted to such specific
 498 contexts in Appendix Figure 7.

499 **B.2 Similarity measures**

500 As mentioned in the Introduction, we utilize the metric Procrustes distance [14] to quantify the
 501 similarity between the hidden states of RNN models, denoted by $H \in \mathbb{R}^{B \times T \times N}$, and the experi-
 502 mentally recorded neural responses, represented as $\tilde{H} \in \mathbb{R}^{B \times T \times N'}$. Here, B represents the number
 503 of trials or experimental conditions, T denotes the number of time steps in each trial, and N and
 504 N' correspond to the number of RNN hidden units and recorded neurons, respectively. The metric
 505 Procrustes distance can be viewed as the residual distance after the two neural representations are
 506 aligned with an optimal rotation, and is quantified as

$$\theta(H, \tilde{H}) = \min_{Q \in \mathcal{O}} \arccos \left(\frac{\langle H^\phi, \tilde{H}^\phi Q \rangle}{\|H^\phi\| \|\tilde{H}^\phi\|} \right) \quad (4)$$

507 where \mathcal{O} is the group of orthogonal linear transformations [15, 87].

508 **B.3 Further details on the neural datasets and synthetic data for RNN training**

509 The **Mante 2013** dataset was downloaded from [https://www.ini.uzh.ch/en/research/](https://www.ini.uzh.ch/en/research/groups/mante/data.html)
 510 [groups/mante/data.html](https://www.ini.uzh.ch/en/research/groups/mante/data.html). We trained RNNs using a synthetic task setup from Neurogym [88],
 511 which included a 350 ms fixation period, a 750 ms stimulus presentation period, a 300 ms delay
 512 period, and a 300 ms decision period. The activity of the trained RNNs during the stimulus period

513 was then compared to the downloaded neural dataset using the aforementioned similarity measures. A
 514 grid search on the fixation and decision interval durations revealed only minor differences in distances
 515 and a consistent trend across learning rules.

516 The **Sussillo 2015** dataset consisted of electrode recordings from primary motor (M1) and dorsal
 517 premotor cortex (PMd) taken while a monkey performed a maze-reaching task consisting of 27
 518 different reaching conditions [21]. To assess the similarity between the neural activity and RNNs
 519 we compared activity from -1450 ms to 400 ms relative to movement onset. The inputs and outputs
 520 to train the models were described in Sussillo et al. 2015, but in brief, for each reach condition
 521 there were 16 inputs and 7 target outputs. The 7 outputs were the electromyographic (EMG) signals
 522 recorded from 7 muscles as the monkey performed a reaching movement. 15 inputs specified the
 523 upcoming reach condition, and were derived from preparatory period neural activity. The remaining
 524 input was a hold-cue that took a value of +1 before movement onset and then a value of 0 to
 525 initiate the movement, whereupon the model generated the 7 EMG signals.

526 **B.4 Further details on the learning rule**

527 This subsection aims to clarify the approximation mechanisms employed by each bio-plausible
 528 learning rule. For comprehensive descriptions, we recommend consulting the detailed references
 529 provided. We begin by expressing the gradient via real-time recurrent learning (RTRL) factorization
 530 (an equivalent but causal alternative to the BPTT factorization of the gradient):

$$\frac{\partial L}{\partial W_{h,ij}} = \sum_{l,t} \frac{\partial L}{\partial h_{l,t}} \frac{\partial h_{l,t}}{\partial W_{h,ij}}, \quad (5)$$

531 The primary challenge with RTRL in terms of biological plausibility and computational efficiency
 532 lies in the term $\frac{\partial h_{l,t}}{\partial W_{h,ij}}$ from the gradient decomposition (Eq. 5). This term tracks all recursive
 533 dependencies of $h_{l,t}$ on the weight $W_{h,ij}$ due to recurrent connections, calculated recursively as:

$$\begin{aligned} \frac{\partial h_{l,t}}{\partial W_{h,ij}} &= \frac{\partial h_{j,t}}{\partial W_{h,ij}} + \sum_m \frac{\partial h_{l,t}}{\partial h_{m,t-1}} \frac{\partial h_{m,t-1}}{\partial W_{h,ij}} \\ &= \frac{\partial h_{l,t}}{\partial W_{h,ij}} + \frac{\partial h_{l,t}}{\partial h_{l,t-1}} \frac{\partial h_{l,t-1}}{\partial W_{h,ij}} + \underbrace{\sum_{m \neq l} W_{h,lm} f'(h_{m,t-1}) \frac{\partial h_{m,t-1}}{\partial W_{h,ij}}}_{\text{involving all weights } W_{h,lm}}. \end{aligned} \quad (6)$$

534 Consequently, $\frac{\partial h_{l,t}}{\partial W_{h,ij}}$ presents a significant challenge for biological plausibility as it includes nonlocal
 535 terms, necessitating knowledge of all other network weights for updating each $W_{h,ij}$. **For a learning
 536 rule to be biologically plausible, all information required to update a synaptic weight must be
 537 physically accessible to that synapse. However, it remains unclear how neural circuits could
 538 make such extensive information readily available to every synapse.**

539 Approaches like **e-prop** [19] and equivalently, **RFLO** [53], address this by truncating the problematic
 540 nonlocal terms in Eq. 6, ensuring that updates to $W_{h,ij}$ follow a three-factor framework — the updates
 541 rely solely on local pre- and post-synaptic activity and a third top-down instructive signal (e.g. from
 542 neuromodulators):

$$\widehat{\frac{\partial h_{l,t}}{\partial W_{h,ij}}} = \begin{cases} \frac{\partial h_{i,t}}{\partial W_{h,ij}} + \frac{\partial h_{i,t}}{\partial h_{i,t-1}} \widehat{\frac{\partial h_{i,t-1}}{\partial W_{h,ij}}}, & l = i \\ 0, & l \neq i \end{cases} \quad (7)$$

543 which yields a much simpler factor than the comprehensive tensor depicted in Eq. 6. This truncation
 544 can be achieved in PyTorch using $h.detach()$, preventing gradient propagation through the recurrent
 545 weights.

546 Putting this together, e-prop can be written in terms of known biological processes including —
 547 eligibility trace e and top-down instructive signals I — as [19]:

$$\Delta W_{h,ij}|_{e-prop} = \sum_t I_{i,t} e_{ij,t}, \quad (8)$$

548 where $I_{i,t} = \frac{\partial L}{\partial h_{i,t}}$ is the top-down instructive signal (e.g. from neuromodulator dopamine, neuronal
 549 firing, etc. [86, 19]) sent to neuron i at time t , and $e_{ij,t} = \widehat{\frac{\partial h_{i,t}}{\partial W_{h,ij}}} = \frac{\partial h_{i,t}}{\partial W_{h,ij}} + \frac{\partial h_{i,t}}{\partial h_{i,t-1}} \widehat{\frac{\partial h_{i,t-1}}{\partial W_{h,ij}}}$ is the

550 eligibility trace for synapse (ij) at time t . This is a three-factor rule, with the pre-and postsynaptic
 551 neuron factors in the eligibility trace as well as a third factor from the instructive signal.

552 Besides eligibility traces and top-down instructive signals, recent transcriptomics data [72] suggest
 553 the presence of widespread cell-type-specific local modulatory signals that could convey additional
 554 information for guiding synaptic weight updates. **ModProp** is developed to incorporate these
 555 processes and restore the gradient terms truncated by e-prop, thereby improving the approximation of
 556 the gradient. Specifically, the ModProp update rule is described as follows [54]:

$$\Delta W_{h,ij}|_{ModProp} \propto I_i \times e_{ij} + \left(\sum_{\alpha \in C} \left(\sum_{l \in \alpha} I_l h'_l \right) \times F_{\alpha\beta} \right) * e_{ij},$$

$$F_{\alpha\beta,s} = \mu^{s-1} (W^s)_{\alpha\beta}, \quad (9)$$

557 where I and e again denote the top-down learning signal and the eligibility trace, respectively.
 558 Here, neuron j belongs to type α , neuron p to type β , and C denotes the set of cell types. $F_{\alpha\beta}$ is
 559 hypothesized to represent type-specific filter taps of GPCRs expressed by cells of type β in response
 560 to precursors secreted by cells of type α . The operator $*$ denotes convolution, and s indexes the filter
 561 taps. The hyperparameter μ , set to 0.25 in this study, and the genetically predetermined $(W^s)_{\alpha\beta}$
 562 values for different filter taps $F_{\alpha\beta,s}$ could be optimized over evolutionary timescales [54].

563 We also explored an older learning rule, **node perturbation** [89, 90], which is known to have trouble
 564 scaling beyond small-scale networks and simple tasks. Specifically, it is implemented by

$$\Delta W_{h,ij}|_{NP} \propto \sum_t \widehat{I}_{i,t} e_{ij,t}, \quad (10)$$

565 where $\widehat{I}_t = (L_t(h_t + \xi) - L_t(h_t))\xi/\sigma^2$ provides an estimate to $\frac{\partial L}{\partial h_t}$; elements of ξ are chosen
 566 independently from a zero-mean Gaussian distribution with variance σ^2 .

567 In addition, we explored **evolutionary strategies** [91] for parameter updates in our model. This
 568 method, for a Gaussian distribution, is implemented as follows:

$$\Delta W_{h,ij}|_{ES} \propto \frac{1}{\sigma S} \sum_{s=1}^S L^{(s)} \epsilon^{(s)}, \quad (11)$$

569 where $\epsilon^{(s)}$ is sampled from a standard normal distribution $\mathcal{N}(0, I)$ for $s = 1, \dots, S$. Here, $L^{(s)}$
 570 represents the loss function evaluated after perturbing the parameter by $\sigma \epsilon^{(s)}$, σ is the standard
 571 deviation of the perturbations, and S is the number of samples. Due to computational constraints, we
 572 set S to 50 for our experiments.

573 B.5 Additional details on training and analysis

574 Our model-data comparison method utilizes Procrustes distances, as implemented in [https://](https://github.com/ahwillia/netrep)
 575 github.com/ahwillia/netrep, with the configuration set to `metric = LinearMetric(alpha =`
 576 `1.0, center_columns = True)`. Additionally, in Appendix Figure 8, we employed Dynamical
 577 Systems Analysis (DSA), available at <https://github.com/mitchellostrow/DSA/tree/main>.
 578 For this analysis, we tested with hyperparameters $n_delays \in \{5, 10, 15, 20\}$ and $rank \in$
 579 $\{10, 20, 30, 40\}$, observing consistent trends across settings. We did not test values beyond these
 580 ranges due to computational resource limitations. For the loss used in training RNNs, we used
 581 cross-entropy loss for the Mante 2013 task and mean-squared error for the Sussillo 2015 task (with
 582 EMG outputs as the targets [92]). As mentioned, the Mante 2013 dataset was downloaded from
 583 <https://www.ini.uzh.ch/en/research/groups/mante/data.html>. However, we obtained
 584 the Sussillo 2015 dataset from the original authors and do not have permission to redistribute it.

585 Our code is available at <https://anonymous.4open.science/r/XYZ2442-860A/>. We utilized
 586 PyTorch Version 1.10.2 [93]. Simulations were executed on a server equipped with two 20-core
 587 Intel(R) Xeon(R) CPU E5-2698 v4 at 2.20GHz. The average training duration for tasks was about 10
 588 minutes, and the analysis pipeline required approximately 2 minutes per model. Training employed
 589 the Adam optimizer. Unless otherwise noted, the learning rate was set at $1e - 3$, optimized through
 590 a grid search of $\{3e - 3, 1e - 3, 3e - 4, 1e - 4\}$. We used a batch size of around 100; changes
 591 in this parameter led to negligible differences in the results. The number of time steps, T , for the

592 Sussillo task was set to 186, matching the original data. The number of time steps T , for the Mante
593 task was 34, based on $dt = 50$ ms from the original Mante paper and the total task duration in the
594 Neurogym setting. Similar trends were observed when we varied dt and the durations of the fixation
595 and delay periods. We employed 200 hidden units for the Sussillo 2015 task and 400 hidden units
596 for the Mante 2013 task; doubling these numbers resulted in similar trends. Each simulation was
597 repeated with four different seeds (except for 10 seeds for Figure 3B), and results for each seed were
598 plotted as separate lines in our figures. Training involved 1000 SGD iterations for Sussillo 2015
599 and 3000 for Mante 2013, with input, recurrent, and readout weights all trainable. Local learning
600 rule approximations were specifically applied to input and recurrent weights, due to the locality
601 issues discussed in Section B.4. Unlike these weights, readout weights do not encounter such issues;
602 hence, by default, the same readout weights were used for both forward and backward computations.
603 However, as verified in Appendix Figure 10, employing random feedback readout weights for training
604 (i.e., feedback alignment [90]) resulted in comparable distances.

605 By default, zero-mean Gaussian noise with a standard deviation of 0.1 was added to the hidden
606 activity, except in cases where the noise was removed to assess its impact. Typically, no connectivity
607 constraints were applied, except for settings in Figure 7B where only 25% of recurrent weights were
608 set as nonzero and trainable, and in Figure 7C where 80% of the neurons were enforced as strictly
609 excitatory and 20% as inhibitory. To enforce Dale’s law, we used the same masking procedure in
610 [18]. To initialize the weights, we initialized with random Gaussian distributions where each weight
611 element $W_{h,ij} \sim \mathcal{N}(0, g^2/N)$, with an initial weight variance of g ; unless otherwise mentioned, we
612 set $g = 1.0$. Input and readout weights were initialized similarly as in [18] (see their *EIRNN.ipynb*
613 notebook).

614 Normalized accuracy, which appears as the x-axis in several plots, is defined such that a value
615 of 1 corresponds to perfect performance. For Sussillo 2015, normalized accuracy is calculated as
616 $1 - \text{normalized mean squared error}$, as used in [94] In the case of Mante 2013, which involves a
617 classification task where mean squared error is not applicable, normalized accuracy is computed
618 as $1 - \text{cross entropy loss}$ to maintain consistency with the definition where 1 indicates the best
619 performance. We also applied x-axis limits to constrain the range between 0 and 1 for uniformity.

620 We detail the data-splitting procedure used for generating the noise floor, i.e. the baseline, in Figure 4.
621 We split the neural data into nonoverlapping groups each containing N_{sample} neurons (*ineurons1*,
622 *ineurons2*). We sample N_{sample} units from the RNN model (*iunits*). We compute the distance
623 between two samples of neural data $d1 = D(\textit{ineurons2}, \textit{ineurons1})$. $d1$ is the lowest we can hope
624 to get given the variability in the neurons that were recorded. We compute the distance between
625 samples of the model and neural data $d2 = D(\textit{iunits}, \textit{ineurons1})$. For each iteration of this
626 procedure we get a new estimate for the distance between the model and data, and the data-to-data
627 distance.

628 **C Additional simulations**

629 In Appendix Figure 5, we examine the top demixed principle components between data and models.
630 In Appendix Figure 6 displays the similarity among models in terms of their pairwise distances and
631 their embeddings across different sampled training snapshots. In Appendix Figure 7, we demonstrate
632 consistent patterns when recurrent noise is removed, sparsity constraints are applied, and Dale’s law
633 is enforced. We also explore ModProp [54], which incorporates cell-type-specific local modulatory
634 signals to reintroduce terms omitted by e-prop; however, as ModProp is effective only under specific
635 conditions (Dale’s law and *ReLU* activation), confining Appendix Figure 7C to these settings. Further
636 analysis of post-training weight eigenspectrums and distances, conducted using Dynamical Similarity
637 Analysis (DSA), reinforces the similarity between BPTT and e-prop, as shown in Appendix Figure 8.

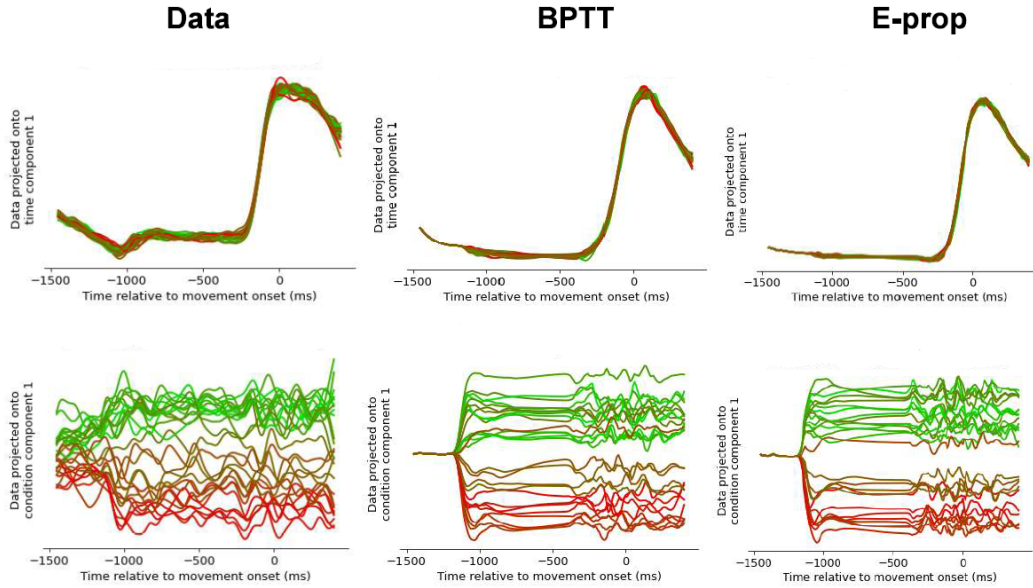


Figure 5: Demixed principle component analysis (dPCA) show qualitative match between model and data when projected onto the time component 1 and condition component 1. Here the Sussillo 2015 dataset is illustrated. Each color represents a different reach condition.

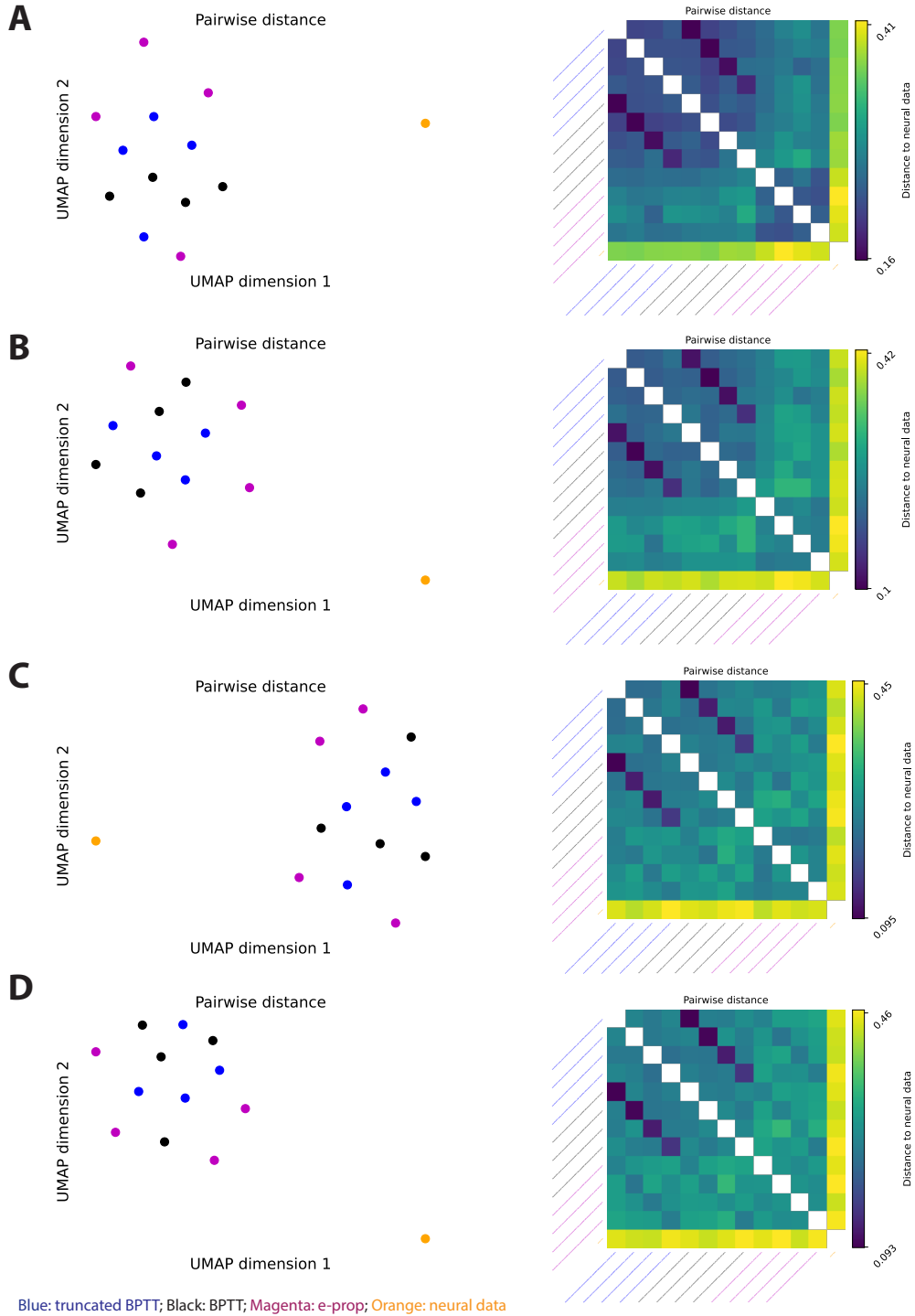


Figure 6: UMAP embedding and pairwise distance matrix heatmap for different models when (A) best e-prop accuracy, (B) 80%, (C) 60%, and (D) 40% accuracies are reached. Here, the Sussillo 2015 dataset is illustrated. Black: BPTT, blue: truncated BPTT, magenta: e-prop, orange: neural data. The pairwise distances show similarities across learning rules relative to data, indicated by lower distances between models as compared to model-data distance.

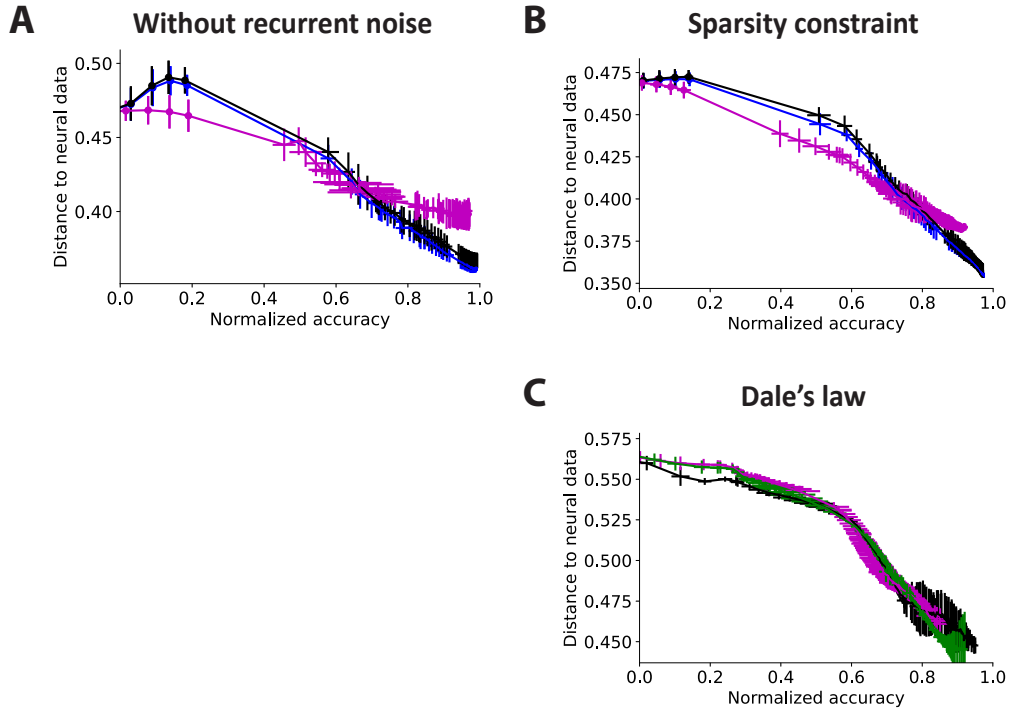


Figure 7: This plot compares Procrustes distances versus accuracy for three learning rules: BPTT (black), e-prop (magenta), and ModProp (green) — the latter functioning exclusively under Dale’s law constraint and *ReLU* activation. Consistent with trends observed in Figure 1, variations include: (A) removal of RNN hidden activity noise, (B) application of a sparsity constraint (limiting to only 25% of the recurrent weights as nonzero and trainable), and (C) enforcement of Dale’s law. The results pertain to the Sussillo 2015 task, with plotting conventions mirroring those in Figure 1.

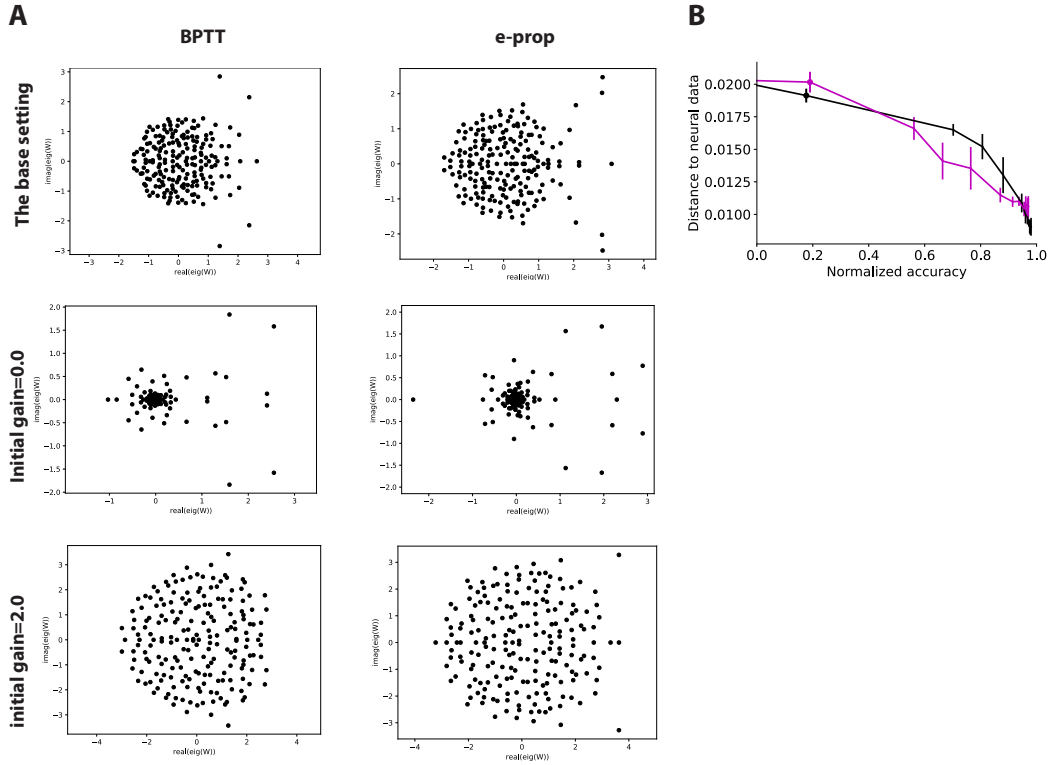


Figure 8: (A) presents the eigenvalues of the recurrent weight matrix post-training, with columns representing BPTT and e-prop respectively. Each row displays a different training setting: the base setting (referenced in Figure 1), initial weight standard deviation set to 0, and initial weight standard deviation set to $2/\sqrt{N}$. Notably, eigenvalue distributions appear more similar within each setting across learning rules (BPTT vs. e-prop) than across different settings for the same learning rule, further highlighting the similarity between BPTT and e-prop. B) The Dynamical Similarity Analysis (DSA), which evaluates systems based on their dynamical characteristics, is also unable to distinguish between learning rules when considering their proximity to neural data.

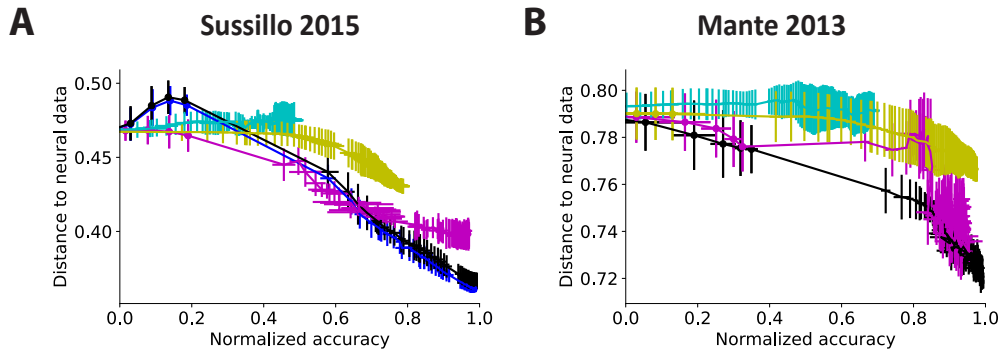


Figure 9: Node perturbation (cyan) and evolutionary strategies (yellow) lead to higher Procrustes distances from the neural data compared to BPTT (black) and e-prop (magenta) when accuracies are equivalent. This figure presents the Procrustes distance versus accuracy plots, adhering to the plotting conventions established in Figure 1, for (A) the Sussillo 2015 task and (B) the Mante 2013 task.

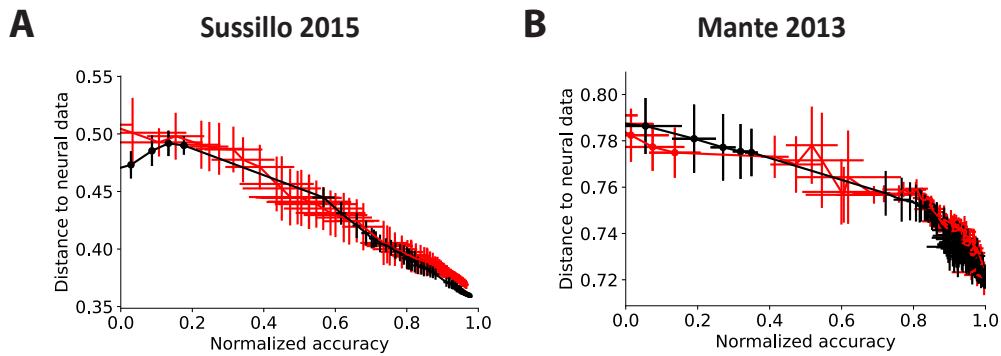


Figure 10: The use of random feedback readout weights for gradient computation (red) resulted in distances comparable to those achieved using exact readout weights (black). Plotting conventions are consistent with those used in previous figures.

638 **NeurIPS Paper Checklist**

639 **1. Claims**

640 Question: Do the main claims made in the abstract and introduction accurately reflect the
641 paper's contributions and scope?

642 Answer: [Yes]

643 Justification: To make this easier for the readers, we have referred to the pertinent figures
644 and sections under "Main contributions" in Introduction.

645 Guidelines:

- 646 • The answer NA means that the abstract and introduction do not include the claims
647 made in the paper.
- 648 • The abstract and/or introduction should clearly state the claims made, including the
649 contributions made in the paper and important assumptions and limitations. A No or
650 NA answer to this question will not be perceived well by the reviewers.
- 651 • The claims made should match theoretical and experimental results, and reflect how
652 much the results can be expected to generalize to other settings.
- 653 • It is fine to include aspirational goals as motivation as long as it is clear that these goals
654 are not attained by the paper.

655 **2. Limitations**

656 Question: Does the paper discuss the limitations of the work performed by the authors?

657 Answer: [Yes]

658 Justification: Details on limitations and future work are discussed in our Discussion section.

659 Guidelines:

- 660 • The answer NA means that the paper has no limitation while the answer No means that
661 the paper has limitations, but those are not discussed in the paper.
- 662 • The authors are encouraged to create a separate "Limitations" section in their paper.
- 663 • The paper should point out any strong assumptions and how robust the results are to
664 violations of these assumptions (e.g., independence assumptions, noiseless settings,
665 model well-specification, asymptotic approximations only holding locally). The authors
666 should reflect on how these assumptions might be violated in practice and what the
667 implications would be.
- 668 • The authors should reflect on the scope of the claims made, e.g., if the approach was
669 only tested on a few datasets or with a few runs. In general, empirical results often
670 depend on implicit assumptions, which should be articulated.
- 671 • The authors should reflect on the factors that influence the performance of the approach.
672 For example, a facial recognition algorithm may perform poorly when image resolution
673 is low or images are taken in low lighting. Or a speech-to-text system might not be
674 used reliably to provide closed captions for online lectures because it fails to handle
675 technical jargon.
- 676 • The authors should discuss the computational efficiency of the proposed algorithms
677 and how they scale with dataset size.
- 678 • If applicable, the authors should discuss possible limitations of their approach to
679 address problems of privacy and fairness.
- 680 • While the authors might fear that complete honesty about limitations might be used by
681 reviewers as grounds for rejection, a worse outcome might be that reviewers discover
682 limitations that aren't acknowledged in the paper. The authors should use their best
683 judgment and recognize that individual actions in favor of transparency play an impor-
684 tant role in developing norms that preserve the integrity of the community. Reviewers
685 will be specifically instructed to not penalize honesty concerning limitations.

686 **3. Theory Assumptions and Proofs**

687 Question: For each theoretical result, does the paper provide the full set of assumptions and
688 a complete (and correct) proof?

689 Answer: [NA]

690
691
692
693
694
695
696
697
698
699
700
701
702
703
704
705
706
707
708
709
710
711
712
713
714
715
716
717
718
719
720
721
722
723
724
725
726
727
728
729
730
731
732
733
734
735
736
737
738
739
740
741
742
743

Justification: This paper does not introduce new theorems or lemmas.

Guidelines:

- The answer NA means that the paper does not include theoretical results.
- All the theorems, formulas, and proofs in the paper should be numbered and cross-referenced.
- All assumptions should be clearly stated or referenced in the statement of any theorems.
- The proofs can either appear in the main paper or the supplemental material, but if they appear in the supplemental material, the authors are encouraged to provide a short proof sketch to provide intuition.
- Inversely, any informal proof provided in the core of the paper should be complemented by formal proofs provided in appendix or supplemental material.
- Theorems and Lemmas that the proof relies upon should be properly referenced.

4. Experimental Result Reproducibility

Question: Does the paper fully disclose all the information needed to reproduce the main experimental results of the paper to the extent that it affects the main claims and/or conclusions of the paper (regardless of whether the code and data are provided or not)?

Answer: [Yes]

Justification: Training details are provided in Appendix B.5. Moreover, our code is available at <https://anonymous.4open.science/r/XYZ2442-860A/>. However, as explained in Appendix B.5 and the *readme.txt* file for our code, it only contains the code to reproduce our Mante 2013 results, as we do not have the permission to redistribute the Sussillo 2015 datasets.

Guidelines:

- The answer NA means that the paper does not include experiments.
- If the paper includes experiments, a No answer to this question will not be perceived well by the reviewers: Making the paper reproducible is important, regardless of whether the code and data are provided or not.
- If the contribution is a dataset and/or model, the authors should describe the steps taken to make their results reproducible or verifiable.
- Depending on the contribution, reproducibility can be accomplished in various ways. For example, if the contribution is a novel architecture, describing the architecture fully might suffice, or if the contribution is a specific model and empirical evaluation, it may be necessary to either make it possible for others to replicate the model with the same dataset, or provide access to the model. In general, releasing code and data is often one good way to accomplish this, but reproducibility can also be provided via detailed instructions for how to replicate the results, access to a hosted model (e.g., in the case of a large language model), releasing of a model checkpoint, or other means that are appropriate to the research performed.
- While NeurIPS does not require releasing code, the conference does require all submissions to provide some reasonable avenue for reproducibility, which may depend on the nature of the contribution. For example
 - (a) If the contribution is primarily a new algorithm, the paper should make it clear how to reproduce that algorithm.
 - (b) If the contribution is primarily a new model architecture, the paper should describe the architecture clearly and fully.
 - (c) If the contribution is a new model (e.g., a large language model), then there should either be a way to access this model for reproducing the results or a way to reproduce the model (e.g., with an open-source dataset or instructions for how to construct the dataset).
 - (d) We recognize that reproducibility may be tricky in some cases, in which case authors are welcome to describe the particular way they provide for reproducibility. In the case of closed-source models, it may be that access to the model is limited in some way (e.g., to registered users), but it should be possible for other researchers to have some path to reproducing or verifying the results.

744
745
746
747
748
749
750
751
752
753
754
755
756
757
758
759
760
761
762
763
764
765
766
767
768
769
770
771
772
773
774
775
776
777
778
779
780
781
782
783
784
785
786
787
788
789
790
791
792
793

5. Open access to data and code

Question: Does the paper provide open access to the data and code, with sufficient instructions to faithfully reproduce the main experimental results, as described in supplemental material?

Answer: [Yes]

Justification: Our code is available at <https://anonymous.4open.science/r/XYZ2442-860A/>. However, as explained in the *readme.txt* file for our code, it only contains the code to reproduce our Mante 2013 results, as we do not have permission to redistribute the Sussillo 2015 datasets.

Guidelines:

- The answer NA means that paper does not include experiments requiring code.
- Please see the NeurIPS code and data submission guidelines (<https://nips.cc/public/guides/CodeSubmissionPolicy>) for more details.
- While we encourage the release of code and data, we understand that this might not be possible, so “No” is an acceptable answer. Papers cannot be rejected simply for not including code, unless this is central to the contribution (e.g., for a new open-source benchmark).
- The instructions should contain the exact command and environment needed to run to reproduce the results. See the NeurIPS code and data submission guidelines (<https://nips.cc/public/guides/CodeSubmissionPolicy>) for more details.
- The authors should provide instructions on data access and preparation, including how to access the raw data, preprocessed data, intermediate data, and generated data, etc.
- The authors should provide scripts to reproduce all experimental results for the new proposed method and baselines. If only a subset of experiments are reproducible, they should state which ones are omitted from the script and why.
- At submission time, to preserve anonymity, the authors should release anonymized versions (if applicable).
- Providing as much information as possible in supplemental material (appended to the paper) is recommended, but including URLs to data and code is permitted.

6. Experimental Setting/Details

Question: Does the paper specify all the training and test details (e.g., data splits, hyper-parameters, how they were chosen, type of optimizer, etc.) necessary to understand the results?

Answer: [Yes]

Justification: Simulation details are provided in Appendix B.5.

Guidelines:

- The answer NA means that the paper does not include experiments.
- The experimental setting should be presented in the core of the paper to a level of detail that is necessary to appreciate the results and make sense of them.
- The full details can be provided either with the code, in appendix, or as supplemental material.

7. Experiment Statistical Significance

Question: Does the paper report error bars suitably and correctly defined or other appropriate information about the statistical significance of the experiments?

Answer: [Yes]

Justification: We tried to provide this information in all applicable figures. This is stated as "The mean is plotted with error bars denoting the standard deviations across four different seeds" in the figure legends.

Guidelines:

- The answer NA means that the paper does not include experiments.

- 794
- 795
- 796
- 797
- 798
- 799
- 800
- 801
- 802
- 803
- 804
- 805
- 806
- 807
- 808
- 809
- 810
- 811
- 812
- The authors should answer "Yes" if the results are accompanied by error bars, confidence intervals, or statistical significance tests, at least for the experiments that support the main claims of the paper.
 - The factors of variability that the error bars are capturing should be clearly stated (for example, train/test split, initialization, random drawing of some parameter, or overall run with given experimental conditions).
 - The method for calculating the error bars should be explained (closed form formula, call to a library function, bootstrap, etc.)
 - The assumptions made should be given (e.g., Normally distributed errors).
 - It should be clear whether the error bar is the standard deviation or the standard error of the mean.
 - It is OK to report 1-sigma error bars, but one should state it. The authors should preferably report a 2-sigma error bar than state that they have a 96% CI, if the hypothesis of Normality of errors is not verified.
 - For asymmetric distributions, the authors should be careful not to show in tables or figures symmetric error bars that would yield results that are out of range (e.g. negative error rates).
 - If error bars are reported in tables or plots, The authors should explain in the text how they were calculated and reference the corresponding figures or tables in the text.

8. Experiments Compute Resources

814 Question: For each experiment, does the paper provide sufficient information on the computer resources (type of compute workers, memory, time of execution) needed to reproduce the experiments?

817 Answer: [Yes]

818 Justification: Information pertaining to computing resources and simulation time can be found in Appendix B.5.

820 Guidelines:

- 821
- 822
- 823
- 824
- 825
- 826
- 827
- 828
- The answer NA means that the paper does not include experiments.
 - The paper should indicate the type of compute workers CPU or GPU, internal cluster, or cloud provider, including relevant memory and storage.
 - The paper should provide the amount of compute required for each of the individual experimental runs as well as estimate the total compute.
 - The paper should disclose whether the full research project required more compute than the experiments reported in the paper (e.g., preliminary or failed experiments that didn't make it into the paper).

9. Code Of Ethics

830 Question: Does the research conducted in the paper conform, in every respect, with the NeurIPS Code of Ethics <https://neurips.cc/public/EthicsGuidelines>?

832 Answer: [Yes]

833 Justification: We have carefully read the NeurIPS Code of Ethics and attest that the research conforms.

835 Guidelines:

- 836
- 837
- 838
- 839
- 840
- The answer NA means that the authors have not reviewed the NeurIPS Code of Ethics.
 - If the authors answer No, they should explain the special circumstances that require a deviation from the Code of Ethics.
 - The authors should make sure to preserve anonymity (e.g., if there is a special consideration due to laws or regulations in their jurisdiction).

10. Broader Impacts

842 Question: Does the paper discuss both potential positive societal impacts and negative societal impacts of the work performed?

844 Answer: [NA]

845 Justification: This research advances our understanding of biologically plausible learning
846 models in recurrent neural networks, with no immediate ethical or societal impacts expected.
847 Over time, the findings could influence related fields like neuroscience and deep learning,
848 potentially affecting society based on how these disciplines evolve.

849 Guidelines:

- 850 • The answer NA means that there is no societal impact of the work performed.
- 851 • If the authors answer NA or No, they should explain why their work has no societal
852 impact or why the paper does not address societal impact.
- 853 • Examples of negative societal impacts include potential malicious or unintended uses
854 (e.g., disinformation, generating fake profiles, surveillance), fairness considerations
855 (e.g., deployment of technologies that could make decisions that unfairly impact specific
856 groups), privacy considerations, and security considerations.
- 857 • The conference expects that many papers will be foundational research and not tied
858 to particular applications, let alone deployments. However, if there is a direct path to
859 any negative applications, the authors should point it out. For example, it is legitimate
860 to point out that an improvement in the quality of generative models could be used to
861 generate deepfakes for disinformation. On the other hand, it is not needed to point out
862 that a generic algorithm for optimizing neural networks could enable people to train
863 models that generate Deepfakes faster.
- 864 • The authors should consider possible harms that could arise when the technology is
865 being used as intended and functioning correctly, harms that could arise when the
866 technology is being used as intended but gives incorrect results, and harms following
867 from (intentional or unintentional) misuse of the technology.
- 868 • If there are negative societal impacts, the authors could also discuss possible mitigation
869 strategies (e.g., gated release of models, providing defenses in addition to attacks,
870 mechanisms for monitoring misuse, mechanisms to monitor how a system learns from
871 feedback over time, improving the efficiency and accessibility of ML).

872 11. Safeguards

873 Question: Does the paper describe safeguards that have been put in place for responsible
874 release of data or models that have a high risk for misuse (e.g., pretrained language models,
875 image generators, or scraped datasets)?

876 Answer: [NA]

877 Justification: This research advances our understanding of biologically plausible learning
878 models in recurrent neural networks, with no immediate ethical or societal impacts expected.
879 Over time, the findings could influence related fields like neuroscience and deep learning,
880 potentially affecting society based on how these disciplines evolve.

881 Guidelines:

- 882 • The answer NA means that the paper poses no such risks.
- 883 • Released models that have a high risk for misuse or dual-use should be released with
884 necessary safeguards to allow for controlled use of the model, for example by requiring
885 that users adhere to usage guidelines or restrictions to access the model or implementing
886 safety filters.
- 887 • Datasets that have been scraped from the Internet could pose safety risks. The authors
888 should describe how they avoided releasing unsafe images.
- 889 • We recognize that providing effective safeguards is challenging, and many papers do
890 not require this, but we encourage authors to take this into account and make a best
891 faith effort.

892 12. Licenses for existing assets

893 Question: Are the creators or original owners of assets (e.g., code, data, models), used in
894 the paper, properly credited and are the license and terms of use explicitly mentioned and
895 properly respected?

896 Answer: [Yes]

897 Justification: Please see Appendix B.5.

898
899
900
901
902
903
904
905
906
907
908
909
910
911
912
913
914
915
916
917
918
919
920
921
922
923
924
925
926
927
928
929
930
931
932
933
934
935
936
937
938
939
940
941
942
943
944
945
946
947
948
949

Guidelines:

- The answer NA means that the paper does not use existing assets.
- The authors should cite the original paper that produced the code package or dataset.
- The authors should state which version of the asset is used and, if possible, include a URL.
- The name of the license (e.g., CC-BY 4.0) should be included for each asset.
- For scraped data from a particular source (e.g., website), the copyright and terms of service of that source should be provided.
- If assets are released, the license, copyright information, and terms of use in the package should be provided. For popular datasets, paperswithcode.com/datasets has curated licenses for some datasets. Their licensing guide can help determine the license of a dataset.
- For existing datasets that are re-packaged, both the original license and the license of the derived asset (if it has changed) should be provided.
- If this information is not available online, the authors are encouraged to reach out to the asset’s creators.

13. New Assets

Question: Are new assets introduced in the paper well documented and is the documentation provided alongside the assets?

Answer: [NA]

Justification: The paper does not release new assets.

Guidelines:

- The answer NA means that the paper does not release new assets.
- Researchers should communicate the details of the dataset/code/model as part of their submissions via structured templates. This includes details about training, license, limitations, etc.
- The paper should discuss whether and how consent was obtained from people whose asset is used.
- At submission time, remember to anonymize your assets (if applicable). You can either create an anonymized URL or include an anonymized zip file.

14. Crowdsourcing and Research with Human Subjects

Question: For crowdsourcing experiments and research with human subjects, does the paper include the full text of instructions given to participants and screenshots, if applicable, as well as details about compensation (if any)?

Answer: [NA]

Justification: The paper does not involve crowdsourcing nor research with human subjects.

Guidelines:

- The answer NA means that the paper does not involve crowdsourcing nor research with human subjects.
- Including this information in the supplemental material is fine, but if the main contribution of the paper involves human subjects, then as much detail as possible should be included in the main paper.
- According to the NeurIPS Code of Ethics, workers involved in data collection, curation, or other labor should be paid at least the minimum wage in the country of the data collector.

15. Institutional Review Board (IRB) Approvals or Equivalent for Research with Human Subjects

Question: Does the paper describe potential risks incurred by study participants, whether such risks were disclosed to the subjects, and whether Institutional Review Board (IRB) approvals (or an equivalent approval/review based on the requirements of your country or institution) were obtained?

Answer: [NA]

950
951
952
953
954
955
956
957
958
959
960
961

Justification: The paper does not involve crowdsourcing nor research with human subjects.

Guidelines:

- The answer NA means that the paper does not involve crowdsourcing nor research with human subjects.
- Depending on the country in which research is conducted, IRB approval (or equivalent) may be required for any human subjects research. If you obtained IRB approval, you should clearly state this in the paper.
- We recognize that the procedures for this may vary significantly between institutions and locations, and we expect authors to adhere to the NeurIPS Code of Ethics and the guidelines for their institution.
- For initial submissions, do not include any information that would break anonymity (if applicable), such as the institution conducting the review.